Specificity in the biosynthesis of the universal tRNA nucleoside N^6-threonylcarbamoyl adenosine (t^6A)—TsaD is the gatekeeper

WILLIAM SWINEHART,[1] CHRISTOPHER DEUTSCH,[1] KATHRYN L. SARACHAN,[2,5] AMIT LUTHRA,[3,6] JO MARIE BACUSMO,[4] VALÉRIE DE CRÉCY-LAGARD,[4] MANAL A. SWAIRJO,[3] PAUL F. AGRIS,[2,7] and DIRK IWATA-REUYL[1]

[1]Department of Chemistry, Portland State University, Portland, Oregon 97201, USA
[2]The RNA Institute, State University of New York, Albany, New York 12222, USA
[3]Department of Chemistry and Biochemistry, and The Viral Information Institute, San Diego State University, San Diego, California 92182, USA
[4]Department of Microbiology and Cell Science, University of Florida, Gainsville, Florida 32611, USA

ABSTRACT

N^6-threonylcarbamoyl adenosine (t^6A) is a nucleoside modification found in all kingdoms of life at position 37 of tRNAs decoding ANN codons, which functions in part to restrict translation initiation to AUG and suppress frameshifting at tandem ANN codons. In Bacteria the proteins TsaB, TsaC (or C2), TsaD, and TsaE, comprise the biosynthetic apparatus responsible for t^6A formation. TsaC(C2) and TsaD harbor the relevant active sites, with TsaC(C2) catalyzing the formation of the intermediate threonylcarbamoyladenosine monophosphate (TC-AMP) from ATP, threonine, and CO_2, and TsaD catalyzing the transfer of the threonylcarbamoyl moiety from TC-AMP to A_{37} of substrate tRNAs. Several related modified nucleosides, including hydroxynorvalylcarbamoyl adenosine (hn^6A), have been identified in select organisms, but nothing is known about their biosynthesis. To better understand the mechanism and structural constraints on t^6A formation, and to determine if related modified nucleosides are formed via parallel biosynthetic pathways or the t^6A pathway, we carried out biochemical and biophysical investigations of the t^6A systems from *E. coli* and *T. maritima* to address these questions. Using kinetic assays of TsaC(C2), tRNA modification assays, and NMR, our data demonstrate that TsaC(C2) exhibit relaxed substrate specificity, producing a variety of TC-AMP analogs that can differ in both the identity of the amino acid and nucleotide component, whereas TsaD displays more stringent specificity, but efficiently produces hn^6A in *E. coli* and *T. maritima* tRNA. Thus, in organisms that contain modifications such as hn^6A in their tRNA, we conclude that their origin is due to formation via the t^6A pathway.

Keywords: N^6-threonylcarbamoyl adenosine; N^6-hydroxynorvalylcarbabamoyl adenosine; RNA modification; kinetics

INTRODUCTION

Nucleoside modification is a hallmark of the post-transcriptional processing of transfer RNA (tRNA), resulting in the introduction of scores of structurally modified nucleosides (Boccaletto et al. 2018). The modification N^6-threonylcarbamoyl adenosine (t^6A), which in some organisms is further modified to a cyclic hydantoin (Miyauchi et al. 2013; Matuszewski et al. 2017), is one of a core group of modified nucleosides that are universally conserved among all organisms (Thiaville et al. 2014). Found exclusively at position-37 in the anticodon loop of ANN decoding tRNA (Fig. 1), t^6A appears to facilitate codon-anticodon interactions by preorganizing the anticodon loop (Stuart et al. 2000; Murphy et al. 2004). In Bacteria t^6A is essential in all but a handful of organisms (Thiaville et al. 2015), due at least in part to serving as an identity element for IleRS, the isoleucine tRNA-synthetase, and TilS, the enzyme responsible for the formation of the modified nucleoside lysidine in the anticodon of $tRNA^{Ile}$. Although not essential in yeast,

[5]**Present address:** Department of Chemistry, Wilson College, Chambersburg, PA 17201, USA
[6]**Present address:** Department of Medicine, University of Connecticut Health Center, Farmington, CT 06030, USA
[7]**Present address:** Department of Medicine—Cardiology, Duke University Medical School, Durham, NC 27710, USA
Corresponding author: iwatareuyld@pdx.edu
Article is online at http://www.rnajournal.org/cgi/doi/10.1261/rna.075747.120.

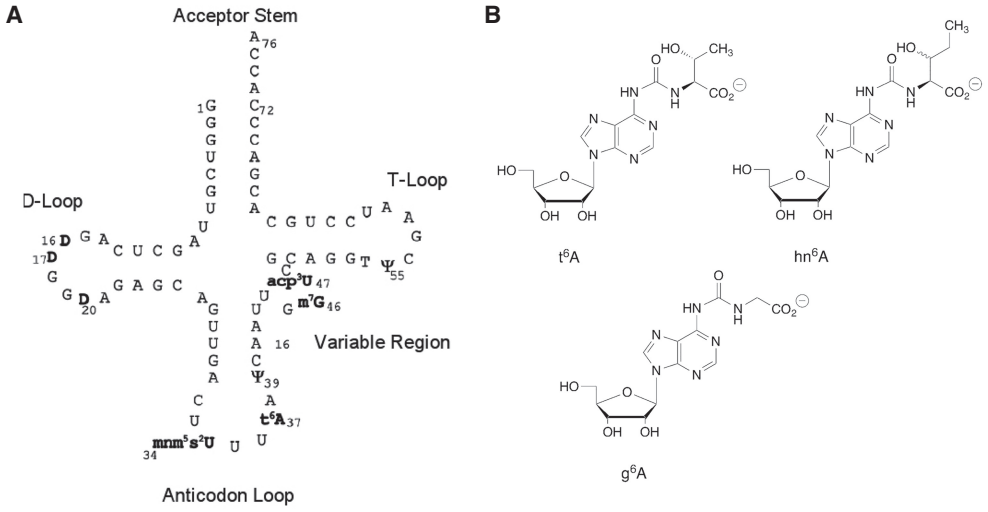

FIGURE 1. tRNA^{Lys}(UUU) from *E. coli* with all of the modifications indicated (*A*), and the structures of t^{6}A, hn^{6}A, and g^{6}A (*B*).

mutants deficient in t^{6}A exhibit severely compromised growth (Thiaville et al. 2016), and display a number of translation related defects (Thiaville et al. 2016), including translation initiation at upstream non-AUG codons and increased frame-shifting in a context dependent manner.

The t^{6}A biosynthetic pathway was first elucidated in Bacteria (Deutsch et al. 2012), and subsequently described in Eukarya and Archaea (Perrochia et al. 2013). The biosynthesis occurs in two steps with the initial formation of threonylcarbamoyldenylate (TC-AMP) (Lauhon 2012), a reaction catalyzed by the enzymes TsaC/TsaC2 in Bacteria (Fig. 2; Thiaville et al. 2014), or Tcs1/Tcs2 in Eukarya and Archaea (Thiaville et al. 2014). The second step involves the transfer of the threonylcarbamoyl moiety to N^6 of adenosine-37 in substrate tRNAs and is catalyzed by the threonylcarbamoyl transferase complex (TCT complex), which is composed of different proteins dependent on the Kingdom (Thiaville et al. 2014). In Bacteria the TCT complex is composed of the proteins TsaB, TsaD, and TsaE (Fig. 2); Archaea and Eukarya utilize the proteins Tcs3, Tcs5, Tcs6, Tcs7, and Tcs8, and in mitochondria the TCT complex is composed of the single protein Tcs4 (Thiaville et al. 2014). Notably, TsaC(C2) and Tcs1(2) are homologs, as are TsaD and Tcs3 (4), and not surprisingly, these two protein families harbor the catalytic sites for the reactions of t^{6}A biosynthesis. Interestingly, homologs of these two families are found fused in the enzyme TobZ (Parthier et al. 2012), which catalyzes the carbamoylation of the antibiotic tobramycin to form nebramycin-5′, a reaction that involves the formation of the intermediate carbamoyl-AMP.

In addition to t^{6}A, two similar modified nucleosides have been reported, N^6-hydroxynorvalylcarbamoyl adenosine (hn^{6}A), discovered in the tRNA of several thermophilic Bacteria and Archaea (Reddy et al. 1992), and N^6-glycinylcarbamoyladenosine (g^{6}A), discovered in yeast tRNA (Fig. 1; Schweizer et al. 1970). Notably, hydroxythreonine has been reported to be a substrate for *E. coli* TsaBCDE (Nagao et al. 2017), suggesting that the t^{6}A system may be responsible for the formation of other naturally occurring modified nucleosides. As part of an effort to better understand the mechanism and structural constraints on t^{6}A formation, and to investigate whether related modified nucleosides can be formed via the t^{6}A pathway, we carried out kinetic and biophysical studies to address the specificity of the bacterial t^{6}A biosynthetic systems from *E. coli* and *Thermotoga maritima*, and report the results of those investigations here.

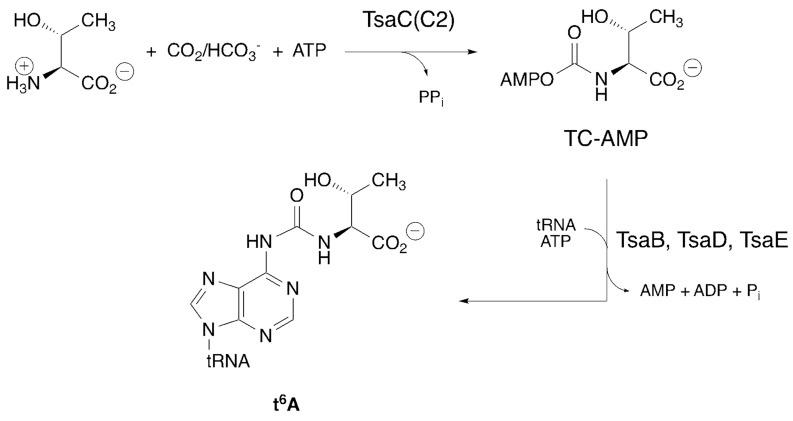

FIGURE 2. The t^{6}A biosynthetic pathway in Bacteria.

RESULTS

Because the t^6A system carries out t^6A biosynthesis in two discrete steps, the TsaC(C2) catalyzed formation of TC-AMP from CO_2/HCO_3^-, threonine, and ATP, followed by the TsaD catalyzed transfer of the TC-unit to tRNA, issues of system specificity are relevant for both steps. In the case of *E. coli* TsaC and *Thermotoga maritima* TsaC2, both enzymes can function in the absence of the TCT complexes, and so can be assayed independently. In contrast, addressing TsaD specificity requires a complete tRNA modification assay with TsaC(C2), and in this case we were necessarily limited in possible TsaD substrates by the TC-AMP analogs that TsaC(C2) were capable of producing. However, because both TsaC and TsaC2 display broader substrate tolerance than TsaD (*vide infra*), this proved not to be a practical limitation.

Characterization of a PP_i continuous spectrophotometric assay for TsaC(C2) activity

Our prior assays of the TsaC(C2) catalyzed formation of TC-AMP were carried out by HPLC, but to facilitate a more extensive kinetic analysis of *E. coli* TsaC and *Thermotoga maritima* TsaC2 we sought to use a more efficient method for quantifying the activity of the enzymes, and settled on indirectly monitoring the formation of the co-product pyrophosphate (PP_i) utilizing a continuous UV-vis assay that couples a PP_i-dependent phosphofructokinase enzyme to NADH oxidation via glycolytic enzymes (O'Brien 1976). To ensure that the PP_i-detection assay would be appropriate for measuring initial velocities of TsaC(C2), we measured the kinetics of PP_i consumption in the absence of TsaC(C2), treating the multienzyme system as a single kinetic species (Supplemental Fig. 1A). The apparent K_M (K_M^{App}) of PP_i for the system was 28.6 μM, with a V_{max}^{App} of 74.2 μM min^{-1}. Since a preliminary kinetic analysis of *E. coli* TsaC using HPLC provided an approximate K_M for threonine and ATP in the low millimolar and high micromolar range, respectively, and a V_{max} of ~0.6 μM min^{-1} (data not shown), the measured parameters of the PP_i-detection assay allowed us to easily establish conditions in which flux through the coupling enzymes was not rate limiting over the range of substrate concentrations that we anticipated investigating (Supplemental Fig. 2), therefore ensuring that the rate measurements of TsaC(C2) would not be compromised using the coupled assay.

Given that ATP is a substrate in the TsaC(C2) reaction, we also needed to confirm that ATP, and other nucleotide triphosphates, would not unduly impact the kinetics of the coupled assay. Measuring initial velocity data over a range of ATP concentrations demonstrated that not unexpectedly, ATP behaved as an inhibitor, and global analysis of the data fit to the nonlinear Michaelis–Menten equations for competitive, uncompetitive, and noncompetitive inhibition systems demonstrated that it functioned as a competitive inhibitor (Supplemental Fig. 1B). Other nucleotide triphosphates behaved similarly (data not shown). Fortunately for our purposes, the K_i value determined for ATP (1.18 mM) was relatively high, and by treating ATP as both substrate and inhibitor in the TsaC(C2) assays we were able to determine the relative kinetic parameters for a variety of amino acids and nucleotide triphosphates (NTPs) that functioned as substrates with *E. coli* TsaC and/or *T. maritima* TsaC2 (*vide infra*).

Steady-state kinetic analysis of *E. coli* TsaC and T. maritima TsaC2

Whereas the complete PP_i-detection assay containing *E. coli* TsaC but lacking threonine exhibited a stable baseline at 340 nm, indicating no reaction of ATP to form PP_i, the *T. maritima* TsaC2 exhibited a slow rate of NADH oxidation in the absence of threonine, suggesting that a low level of uncoupling of the reaction was occurring; this background rate was calculated for each concentration of ATP (or other NTPs) used and subtracted from the experimentally measured rates in the kinetic assays.

Steady-state analysis provided kinetic values for both *T. maritima* TsaC2 and *E. coli* TsaC enzymes with various amino acids and NTPs. To appropriately account for the inhibition of the coupled system observed with nucleotide triphosphates, ATP was treated as a noncompetitive inhibitor in the assays in which amino acids were varied according to the simplified Michaelis–Menten equation for noncompetitive inhibition (Segel 1975),

$$v = \frac{V_{max}[aa]}{\alpha(K_M + [aa])}$$

where $\alpha = \left(1 + \frac{[ATP]}{K_i}\right)$, K_i is the inhibition constant of ATP, and aa is the relevant amino acid being investigated. This is essentially equivalent to the reduced equation for a multisubstrate reaction in which a nonvaried substrate also serves as an inhibitor. In assays with variable NTP the system can be treated as one subject to substrate inhibition (Segel 1975), and the data fit to the following simplified Michaelis–Menten equation for substrate inhibition:

$$v = \frac{V_{max}[NTP]}{K_M + \alpha[NTP]}$$

where $\alpha = \left(1 + \frac{[NTP]}{K_i}\right)$, and K_i is the inhibition constant of the NTP being investigated. It is important to recognize that due to the limited kinetic analysis carried out here, the kinetic constants determined for both amino acids and NTPs are not the intrinsic constants, but they do serve as a direct measure of the relative values between substrates, and therefore provide quantitative information on

TABLE 1. Kinetic parameters for *E. coli* TsaC with various amino acids

Substrate	k_{cat} (min^{-1})	K_m (mM)	k_{cat}/K_m (K_m^{-1} min^{-1})
Thr	0.813 ± 0.065	3.66 ± 1.00	0.222 ± 0.160
hnV[a]	0.592 ± 0.038	4.53 ± 0.746	0.131 ± 0.105
Ser	0.831 ± 0.042	7.65 ± 1.04	0.109 ± 0.091
Gly	---[b]	---	---
Val	---	---	---
Ala	---	---	---

[a]Kinetic parameters assuming only on the L-enantiomer of racemic hnV serves as a substrate.
[b]Enzymatic activity not detected.

the ability of various amino acids and NTPs to serve as substrates for TsaC and TsaC2.

Both *E. coli* TsaC and *T. maritima* TsaC2 exhibited relaxed substrate specificity toward amino acids, and were able to form TC-AMP analogs using several amino acids that contain a hydroxyl-group bound to the β-carbon (Tables 1, 2; Fig. 3). Interestingly, aliphatic amino acids lacking a hydroxyl group, even those of the same or smaller size than threonine, did not function as substrates (Tables 1, 2). *E. coli* TsaC exhibited a k_{cat}/K_M for threonine roughly twofold higher than that for serine and hydroxynorvaline (Table 1), whereas *T. maritima* TsaC2 exhibited much higher selectivity for threonine, exhibiting k_{cat}/K_M for threonine almost an order of magnitude greater than that for serine, and approximately fourfold greater than that for hydroxynorvaline (Table 2).

We next tested the ability of *E. coli* TsaC and *T. maritima* TsaC2 to form TC-AMP analogs with NTPs other than ATP, and both enzymes were able to utilize several NTPs as effective substrates. As observed for ATP, *T. maritima* TsaC2 exhibited a low background rate of NADH oxidation with several NTPs (dATP and GTP) in the absence of threonine, indicating reaction uncoupling with the production of PP_i, but this rate was even lower than that observed with ATP. Control assays of *E. coli* TsaC with various NTPs in the absence of threonine exhibited no uncoupling, consistent with the lack of uncoupling with ATP. Surprisingly, *E. coli* TsaC formed a TC-dAMP intermediate as efficiently as the canonical TC-AMP (Table 3; Fig. 4). Furthermore, all other NTPs with the exception of UTP, dTTP, and CTP were substrates for *E. coli* TsaC, with catalytic efficiencies only three to four times lower than that of ATP (Table 3; Fig. 4). UTP and dTTP did not serve as substrates, whereas CTP served as a substrate (Fig. 4), but displayed a profile that was poorly fit by the kinetic model, and so kinetic parameters were not extracted from the analysis.

Although *T. maritima* TsaC2 was also able to utilize nucleotide triphosphates other than ATP, it exhibited far higher selectivity for ATP, with a k_{cat}/K_M 100-fold higher than dATP and at least 25-fold higher than any other NTP (Table 4; Fig. 5). This difference was largely attributable to the low K_M for ATP exhibited by TsaC2, which was 10–60× lower than for other NTPs, and 20× lower than the K_M determined for ATP with TsaC.

Transfer of various TC-AMP analogs to tRNA by the TCTC of *E. coli* and *T. maritima*

Having established that both TsaC and TsaC2 are capable of synthesizing TC-AMP analogs comprising various amino acids and nucleotide components, we sought to determine whether these intermediates could serve as substrates for the TCT complex and generate modified tRNA products. To address this question we assayed the full t^{6}A biosynthetic systems (TsaC(C2), TsaB, TsaD, TsaE) for their ability to modify tRNA using our standard radiochemical based tRNA precipitation assay (Deutsch et al. 2012).

When *E. coli* TsaC and the TCT complex were reacted with the three amino acids shown above to serve as substrates for TsaC (threonine, hydroxynorvaline, and serine), only threonine and hydroxynorvaline were observed to serve as substrates for the modification of tRNA (Fig. 6A), indicating that TsaD is more stringent than TsaC and that specificity in the biosynthetic system occurs at the transfer step catalyzed by TsaD. Similarly, the *T. maritima* system (TsaC2 and the TCT complex) was able to utilize threonine and hydroxynorvaline but not serine, efficiently producing both t^{6}A and hn^{6}A modified tRNA, respectively (Fig. 6B).

Consistent with the results above with alternate amino acid substrates, the *T. maritima* system exhibited high

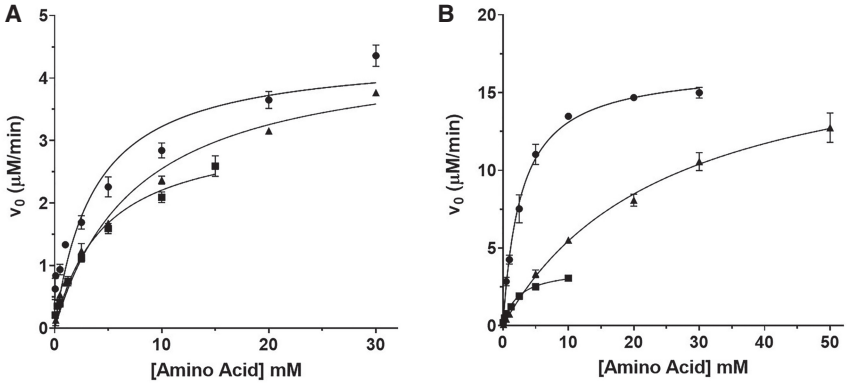

FIGURE 3. Michaelis–Menten plots of *E. coli* TsaC (*A*) and *T. maritima* TsaC2 (*B*) with the amino acids threonine (•), hnV (■), and Ser (▲). Error bars represent standard errors.

TABLE 2. Kinetic parameters for *T. maritima* TsaC2 with various amino acids

Substrate	k_{cat} (min^{-1})	K_m (mM)	k_{cat}/K_m (K_m^{-1} min^{-1})
Thr	3.08 ± 0.060	2.76 ± 0.198	1.12 ± 1.02
hnV[a]	0.68 ± 0.030	2.26 ± 0.274	0.30 ± 0.23
Ser	3.51 ± 0.152	24.8 ± 2.26	0.14 ± 0.12
Gly	---[b]	---	---
Val	---	---	---
Ala	---	---	---

[a]Kinetic parameters assuming only on the L-enantiomer of racemic hnV serves as a substrate.
[b]Enzymatic activity not detected.

selectivity for the nucleotide moiety of the TC-XMP intermediate, producing t^6A-modified tRNA only when ATP was used (Fig. 7). The *E. coli* system also exhibited high selectivity, although it was able to utilize dATP, albeit far less effectively than ATP (Fig. 8), and no other NTPs were able to support formation of t^6A.

NMR saturation transfer experiments with Tsa proteins from *E. coli* and *T. maritima*

To gain further insight into the binding of amino acids to TsaC(C2) and TsaD, saturation transfer difference NMR (STD NMR) was used to probe the affinity of TsaC(C2) and TsaD proteins for threonine and hydroxynorvaline. In these STD NMR experiments, nonexchangeable protons on the amino acid that are located within 5 Å of TsaC(C2) or TsaD exhibit STD NMR peaks. Distinct proton peaks from the Hβ, Hα, and Hγ protons of threonine (Fig. 8A,C) are visible when *E. coli* TsaC interacts with this amino acid, indicating spatial proximity of those protons to the enzyme and consistent with a binding event. Similarly, distinct peaks from the Hβ and Hα protons of hydroxynorvaline (Fig. 8B,D) are visible, along with a weak signal for Hδ. *E. coli* TsaD shows a similar pattern of interaction with threonine (Fig. 8A,C), but evidence of its interaction with hydroxynorvaline is limited to a Hβ peak and a weaker Hδ peak (Fig. 8B,D), suggesting a more spatially limited interaction. Distinct STD NMR peaks are visible from the Hβ and Hγ protons of threonine and the Hα, Hβ, and Hδ protons of hydroxynorvaline to *T. maritima* TsaC2 (Fig. 8), again suggesting spatial proximity and binding events between TsaC2 and both amino acids. Although *T. maritima* TsaD was not as well behaved under NMR conditions as the other three enzymes, making data collection difficult, it was nevertheless possible to obtain a clear STD NMR signal for its interaction with the Hβ proton of threonine along with a weaker one for the Hγ proton. In the case of its interaction with hydroxynorvaline, distinct signals due to interactions with the Hα and Hβ protons were clearly visible, as well as weaker signals from its interaction with the Hγ and Hδ protons (Fig. 8B,D). Overall, the *E. coli* proteins exhibited stronger interactions with threonine than with hydroxynorvaline, whereas the *T. maritima* proteins were reversed, exhibiting stronger interactions with hydroxynorvaline than with threonine.

DISCUSSION

To address the specificity of bacterial t^6A biosynthesis we investigated the kinetics of two prototypic bacterial systems, that from *E. coli*, which utilizes TsaC for the formation of the intermediate TC-AMP, and from *T. maritima*, which utilizes TsaC2. Although both systems share homologous TsaB, TsaD, and TsaE proteins, which together form the TCT complexes, these assemble into distinct quaternary complexes; the *E. coli* system forms both a TsaBD heterodimer and a TsaBDE heterotrimer (Zhang et al. 2015), whereas the *T. maritima* system forms a TsaBD complex with 2:2 stoichiometry and TsaBDE complexes with 2:2:1 and 2:2:2 stoichiometry (Luthra et al. 2018).

It is important to note that although the kinetic studies of the alternate amino acids and NTPs carried out with TsaC and TsaC2 provide a direct measure of the relative activity of the enzymes with the various substrates, the same is not true for the tRNA modification assays (Figs. 6, 7). For the amino acids and nucleotides tested, the "normal" substrates (threonine and ATP) are more efficient with TsaC and TsaC2, and TC-AMP is produced faster in the t^6A assays than the other amino acid or nucleotide analogs of TC-AMP, so the rates of modified tRNA formation using the various amino acids and (d)NTPs cannot be compared directly. Furthermore, multiple turnovers of the *T. maritima* TCT complex require ATP hydrolysis by TsaE (Luthra et al. 2018), and although we have shown that *T. maritima* TsaE can utilize dATP efficiently (Luthra et al. 2019), it is unknown if other NTPs are also accepted by TsaE, and thus if the *T. maritima* TCT is capable of multiple turnovers

TABLE 3. Kinetic parameters for *E. coli* TsaC with various nucleotides

Substrate	k_{cat} (min^{-1})	K_m (mM)	k_{cat}/K_m ($K_m^{-1}min^{-1}$)
ATP	0.53 ± 0.05	0.831 ± 0.126	0.632 ± 0.499
GTP	0.30 ± 0.05	1.01 ± 0.243	0.300 ± 0.204
CTP	***[a]	***	***
UTP	---[b]	---	---
dATP	0.58 ± 0.07	0.913 ± 0.192	0.632 ± 0.453
dGTP	0.49 ± 0.43	2.62 ± 2.71	0.185 ± 0.012
dCTP	0.18 ± 0.08	0.90 ± 0.69	0.200 ± 0.061
dTTP	---	---	---

[a]Fit was ambiguous.
[b]Enzymatic activity not detected.

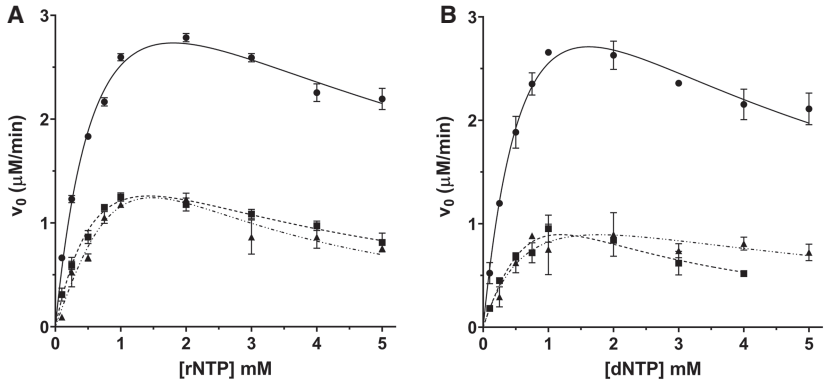

FIGURE 4. Michaelis–Menten plots of *E. coli* TsaC with rNTPs (*A*) and dNTPs (*B*). ATP/dATP (•), GTP/dGTP (■), and CTP/dCTP (▲). Error bars represent standard errors.

with (d)NTPs other than (d)ATP. Nevertheless, because the *T. maritima* TCT complex can carry out a single turnover in the absence of ATP (Luthra et al. 2018), and the assays were carried out with high protein concentration, we were easily able to detect the formation of product corresponding to less than one turnover. So although data from the full modification assays do not provide quantitative rate information, the data do provide a qualitative measure of the ability of the TCT complexes to accept TC-AMP analogs in the modification of tRNA. Therefore, we can conclude that amino acids and NTPs that do not support tRNA modification in these assays are not accepted efficiently as substrates by the relevant TCT complex.

Although TC-AMP analogs comprised of alternate nucleotides, if accepted by TsaD, would not impact the overall formation of t^{6}A$_{37}$ as only the TC unit is transferred to the tRNA, the TsaD proteins exhibited specificity for AMP, and to a lesser extent dAMP in the case of *E. coli* TsaD, as the nucleotide moiety. However, the fact that both TsaC and TsaC2 were able to produce a variety of TC-AMP nucleotide analogs in our in vitro assays does not imply that such intermediates are generated to any significant extent in the cell; indeed, the measured K_M values for all (d)NTPs except ATP are far above their cellular concentrations (Bochner and Ames 1982; Buckstein et al. 2008), which with the exception of ATP (~3.5 mM) and GTP (~1.5 mM) are in the mid- to low micromolar range, whereas the K_M values for ATP indicate that both enzymes are likely saturated with this substrate in vivo.

In conclusion, we have shown that both TsaC and TsaC2, which produce the intermediate TC-AMP in t^{6}A biosynthesis, are highly promiscuous in both their amino acid and NTP substrates, but that TsaD, a component of the TCT complex in t^{6}A biosynthesis and the catalytic subunit responsible for transferring the TC moiety of TC-AMP to A$_{37}$ of tRNA, exhibits much more selectivity, accepting only TC- and hnC-AMP as efficient substrates. The STD NMR experiments are broadly consistent with these activity measurements, and indicate that TsaC(C2) and TsaD form active sites that bind both threonine and hydroxynorvaline in isolation from the other reactants, and in the case of TsaD in the absence of the other components of the TCT complex.

Comparison of the TC-transfer sites of *E. coli* and *T. maritima* TsaD as seen in their crystal structures in complex with other Tsa proteins (PDB ID 4YDU, Zhang et al. 2015; and PDB ID 6N9A, Luthra et al. 2019, respectively) reveals that both have identical active site residues. However, because these structures represent different steps in the t^{6}A cycle, the TsaD subunits in these structures exhibit significantly different conformations in and around the active site region due to a TsaE-induced upward movement of a helix-loop-helix (lever arm) in the *T. maritima* structure, which renders the TC-transfer site more accessible in that structure (Luthra et al. 2019). To enable a meaningful comparison of the active sites, we generated a homology model of *E. coli* TsaD with the lever arm in the "up" position and compared it with *T. maritima* TsaD as seen in the crystal structure 6N9A (Supplemental Fig. 3). This shows that the *T. maritima* TsaD active site is ~18% larger than that of the *E. coli* enzyme (950 Å^3 vs. 804 Å^3), a difference that may account for the somewhat greater efficiency for hnC-AMP exhibited by the *T. maritima* TsaD (Fig. 6).

To gain insight into the structural basis of recognition of hnC- and TC-AMP by TsaD, and the failure of SC-AMP to serve as an efficient substrate, we docked both TC-AMP and hnC-AMP in the active site of *T. maritima* TsaD as seen in the 6N9A crystal structure (Luthra et al. 2019) using H-Dock (Yan et al. 2017). The ligands were docked based on the position of the crystallographically observed carboxy-AMP bound in that structure as well as template free, and in both cases the models show (Fig. 9; Supplemental Fig. 4) that the amino acid hydroxyl groups of

TABLE 4. Kinetic parameters for *T. maritima* TsaC2 with various nucleotides

Substrate	k_{cat} (min^{-1})	K_m (mM)	k_{cat}/K_m (K_m^{-1} min^{-1})
ATP	1.97 ± 0.18	0.041 ± 0.012	48.54 ± 34.1
GTP	0.673 ± 0.157	0.380 ± 0.142	1.77 ± 0.990
CTP	1.58 ± 0.226	1.48 ± 0.273	1.07 ± 0.772
UTP	0.748 ± 0.411	0.673 ± 0.460	1.18 ± 0.308
dATP	0.424 ± 0.061	0.824 ± 0.200	0.515 ± 0.354
dGTP	0.443 ± 0.349	2.35 ± 2.2	0.189 ± 0.020
dCTP	---[a]	---	---
dTTP	---	---	---

[a]Enzymatic activity not detected.

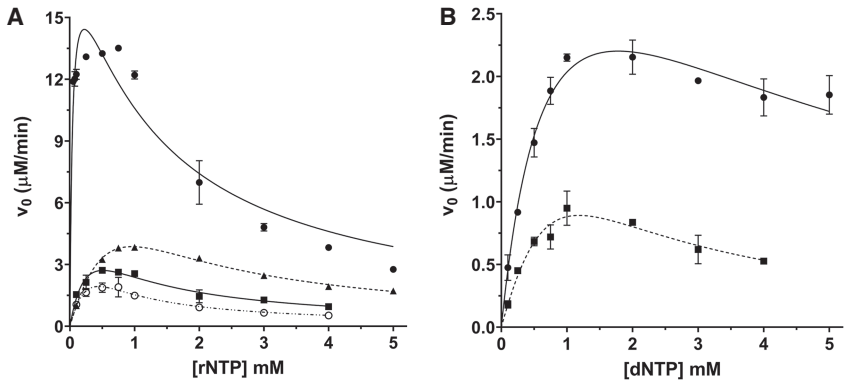

FIGURE 5. Michaelis–Menten plots of *T. maritima* TsaC2 with rNTPs (*A*), and dNTPs (*B*). ATP/dATP (•), GTP/dGTP (■), and CTP (▲), and UTP (○). Error bars represent standard errors.

TC-AMP and hnC-AMP are coordinated by the conserved side chain of Glu12, whereas the C_γ or $C_\gamma C_\delta$ atoms of Thr or hnV, respectively, are within van der Waals contact distance from C_β of Cys10. Evidence for these interactions are also seen in the STD NMR experiments, where peaks due to C_γ, and C_δ in the case of hnC-AMP, are visible. The absence of a C_γ interaction may account for the failure of SC-AMP to serve as an efficient substrate for TsaD as this would give more mobility to the SC- moiety and may in turn compromise optimal positioning of its carbonyl group for nucleophilic attack by N6 of A_{37}.

The ability of the t^6A biosynthetic systems investigated here to efficiently produce hn^6A modified tRNA, together with the previous report of hn^6A in *T. maritima* tRNA (Reddy et al. 1992) and the recent discovery that hn^6A is located at position-37 of several ANN-decoding *Methanocaldococcus jannaschii* tRNA (Yu et al. 2019), suggests that the *T. maritima* t^6A_{37} system, and that of other organisms in which hn^6A has been found (Reddy et al. 1992) functions as the biosynthetic machinery responsible for this modification. Although the metabolic origin of hydroxynorvaline is unknown, the function of hn^6A presumably mimics that of t^6A, and given that hn^6A has only been found in thermophiles, it may be that the ethyl moiety, which provides a larger hydrophobic surface than the methyl moiety of t^6A, better stabilizes the anticodon loop structure necessary for efficient codon binding (Murphy et al. 2004).

MATERIALS AND METHODS

General

Buffers, salts, and reagents (highest quality grade available) were purchased from Sigma-Aldrich. NTPs and dNTPs used in kinetic studies were from Fisher Scientific, and were ≥99% pure and certified free of contaminating nucleotide triphosphates. Amino acids used were from Millipore Sigma, and were at least ≥98% pure; NMR analysis of hydroxynorvaline and serine showed them to be free of contaminating threonine. Dithiothreitol (DTT), isopropyl-β-D-thiogalacto-pyranoside (IPTG), kanamycin sulfate, diethylpyrocarbonate (DEPC), and ampicillin were purchased from RPI Corporation. [U-^{14}C]-threonine and [U-^{14}C]-sodium bicarbonate were obtained from PerkinElmer or Moravek Inc. Amicon Ultra 15 and 0.5 centrifugal filter units and NovaBlue Singles competent cells were acquired from EMD Millipore. Nickel-nitrilotriacetic acid agarose (Ni^{2+}-NTA agarose) and Whatman GF-B PVDF syringe filters were purchased from Fisher Scientific. GeneJet Plasmid Miniprep kits and PageRuler prestained protein ladder were purchased from Fermentas. Dialysis was carried out in Slide-A-Lyzer cassettes (Thermo Fisher Scientific). All reagents for sodium dodecyl sulfate polyacrylamide gel electrophoresis (SDS-PAGE) were purchased from Bio-Rad. SDS-PAGE analysis was carried out using 12% gels and visualized with Coomassie Brilliant Blue. Diethylpyrocarbonate-treated water was used in the preparation of all solutions for RNA-related assays.

Instrumentation

Ultraviolet-visible (UV-Vis) spectrophotometry was performed with a Varian Cary 100 spectrophotometer equipped with a thermostatted multicell holder. Liquid scintillation counting (LSC) was conducted with a Hidex 300 SL counter. HPLC was carried out with an Agilent 1100 system equipped with a UV-Vis diode array detector. Nuclear magnetic resonance spectra were collected at 37°C on a Bruker Avance 700 MHz spectrometer equipped with a z-gradient TXI cryoprobe.

Purification of proteins and preparation of RNA

The purification of *E. coli* TsaB, TsaC, TsaD, and TsaE was carried out as described previously (Deutsch et al. 2012). The *T. maritima* TsaC2, TsaB, TsaD, and TsaE proteins were purified as described

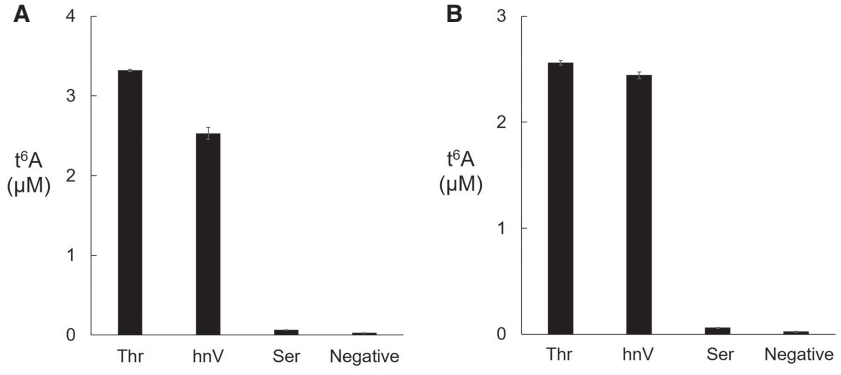

FIGURE 6. t^6A modified tRNA formed by either the *E. coli* (*A*) or *T. maritima* (*B*) biosynthetic systems in the presence of various amino acids. Error bars represent standard errors.

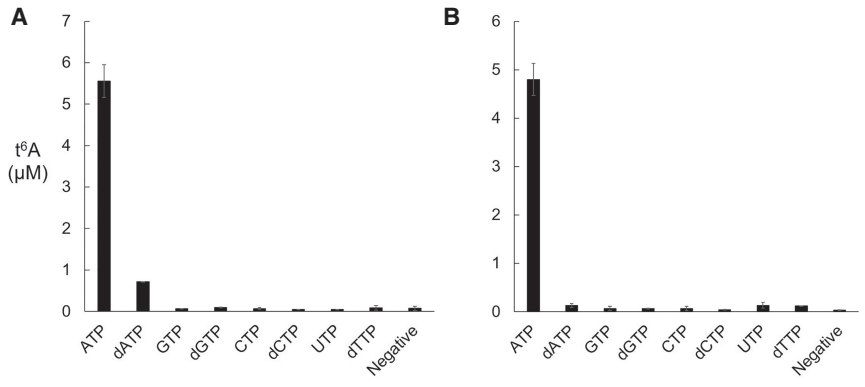

FIGURE 7. t^{6}A modified tRNA formed by either *the E. coli* (*A*) or *T. maritima* (*B*) biosynthetic systems in the presence of various rNTPs or dNTPs. Error bars represent standard errors.

(Luthra et al. 2018). The transcript for *E. coli* tRNA^{Lys} was prepared and purified as previously described (Deutsch et al. 2012).

Steady state kinetics of *E. coli* TsaC—HPLC analysis

Kinetic assays contained 50 mM MOPS (pH 7.4), 50 mM KCl, 0.5 mM $MgCl_2$, 5 μM TsaC, and variable L-threonine (50 μM–50 mM) and 10 mM ATP when analyzing L-threonine kinetics, or 10 mM L-threonine and variable ATP (100 μM–10 mM) when analyzing ATP kinetics. All assays contained 20 mM sodium bicarbonate (pH 7.4); rigorous kinetic analysis of *E. coli* TsaC as a function of sodium bicarbonate concentration has not been carried out, but the mitochondrial enzyme displays a K_M of 13 mM (Lin et al. 2018), and the full *E. coli* t^{6}A system exhibits >80% of full activity at 20 mM sodium bicarbonate.

Reactions were carried out at 37°C for 5–30 min, terminated by centrifugal filtration (Millipore centrifugal filter units, 10 kDa cutoff) for 30 sec to remove TsaC, and analyzed by HPLC using a Supelco Discovery HS C18 (250 Å ~ 2.1 mm, 5 μM) column with a mobile phase of 10 mM ammonium acetate (pH 6.0) and acetonitrile at a flow rate of 0.3 mL/min. After a five-minute hold with ammonium acetate buffer a linear gradient to acetonitrile (100:0 to 60:40 over 20 min) was applied. Initial velocities were calculated from time-course data of peak areas (collected in triplicate) and fit to the Michaelis–Menten equation using Kaleidagraph.

Validation of pyrophosphate continuous assay

Reactions using the pyrophosphate assay (Sigma-Aldrich P7275) were performed in a final volume of 150 μL containing 50 μL of the pyrophosphate reagent prepared according to the manufacturer's instructions. The final concentrations of all assay components were 50 mM MOPS (pH 7.4), 50 mM KCl, 20 mM sodium bicarbonate (pH 7.4), 1.17 mM $MgCl_2$, 15 mM imidazole, 1.67 mM citrate, 30 μM EDTA, 70 μM Mn^{2+}, 10 μM Co^{2+}, 270 μM NADH, 4.0 mM fructose-6-phosphate, 1.67 mg/mL BSA, 1.67 mg/mL sugar stabilizer, 0.026 units PPi-dependent phosphofuctokinase, 0.375 units aldolase, 2.5 units triosephosphate isomerase, and 0.25 units glycerophosphate dehydrogenase. Reaction rates for the conversion of NADH to NAD^+ were measured at variable concentrations of pyrophosphate (10 μM to 2 mM). Assays were performed in triplicate at 37°C and monitored spectrophotometrically at an absorbance of 340 nm for 5 min. Initial velocities were calculated from the time-course data and fit to the nonlinear Michaelis–Menten equation using GraphPad Prism 8.

To measure inhibition of the assay by nucleotides, assays were carried out under the conditions described above with the addition of various nucleotide triphosphates in concentrations ranging from 500 μM to 5 mM. The data were globally fit to the nonlinear Michaelis-Menten equations for competitive, uncompetitive, and noncompetitive inhibition using GraphPad Prism 8 to determine a best fit.

Steady state kinetic analysis of *E. coli* TsaC and *T. maritima* TsaC2

Kinetic analysis of the *E. coli* TsaC and *T. maritima* reactions were carried out using the continuous UV-vis coupled

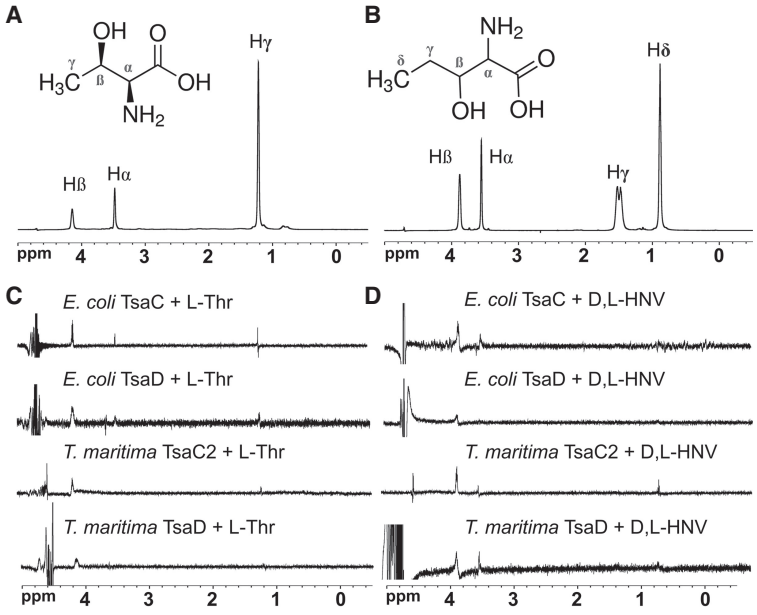

FIGURE 8. Amino acid interaction with the TsaC, TsaC2 and TsaD proteins from *E. coli* and *T. maritima* by saturation difference transfer (STD) NMR. Atomic structure and ^{1}H NMR reference spectra of L-threonine (*A*) and D,L-3-hydroxynorvaline (*B*), with protons and associated resonances labeled. STD NMR spectra of TsaC, TsaC2, and TsaD in complex with L-threonine (*C*) and D,L-3-hydroxynorvaline (*D*) at a 50:1 molar ratio.

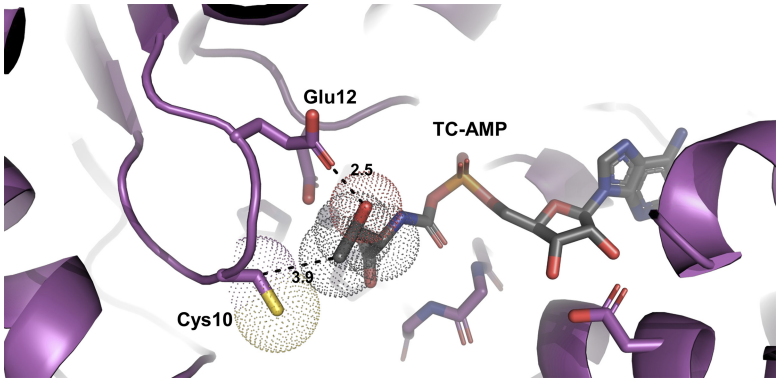

FIGURE 9. Docking model of TC-AMP onto the active site of *T. maritima* TsaD showing interactions with conserved residues Glu12 and Cys10. Atomic van der Waals surfaces are shown as dotted surfaces. The Zn^{2+} ion is shown as a purple sphere. Distances are in Angstroms. The AMP and carbonyl moieties occupy the same sites as the corresponding moieties in carboxy-AMP bound in the crystal structure of *T. maritima* $TsaB_2D_2E_2$ (PDB ID 6N9A).

pyrophosphate assay described above. Assays were performed at a final volume of 150 µL as described. In addition to the components listed above, assays contained 10 µM TsaC or TsaC2, 50 µM–20 mM amino acid (L-threonine, L-serine, D,L-3-hydroxynorvaline, glycine, L-alanine, L-valine), and 1.0 mM ATP when analyzing amino acid kinetics, or 10 mM L-threonine and variable nucleotide triphosphates (50 µM–4.0 mM) when analyzing nucleotide kinetics. Assays were conducted at 37°C and monitored spectrophotometrically at an absorbance of 340 nm for 15 min. TC-AMP concentrations were calculated from the absorbance data based on a stoichiometry of one mole of pyrophosphate consumed per two moles of NADH ($\varepsilon = 6220\ M^{-1}\ cm^{-1}$) oxidized. The data were collected in triplicate and fit to the Michaelis–Menten equation for noncompetitive inhibition by ATP when investigating amino acid kinetics, and to the Michaelis–Menten equation with substrate inhibition when investigating the reaction with various nucleotide triphosphates. Data analysis was carried out using GraphPad Prism 8. In the case of *T. maritima* TsaC2, the background rate of NADH oxidation due to TsaC2 uncoupling in the absence of threonine at each nucleotide triphosphate concentration was subtracted from the raw data for each run before the initial velocity values were calculated.

E. coli t^6A assays with amino acids and nucleotides

Assays probing the transfer of *N*-carbamoyl amino acids to tRNA via the full *E. coli* t^6A biosynthetic system were performed using in vitro transcribed *E. coli* $tRNA^{Lys}(UUU)$ with [^{14}C]-labeled sodium bicarbonate as the source of label, added to a concentration of 150 µM (1,000,000 dpm/assay). Assays were performed in 100 mM Tris (pH 7.5), 300 mM KCl, 5 mM DTT, 20 mM $MgCl_2$, 10 mM amino acid, 50 µM *E. coli* $tRNA^{Lys}$ transcript, 2 mM ATP, and 2.0 µM each *E. coli* TsaB, TsaC, TasD, and TsaE. Assays were incubated at 37°C for 1 h, then quenched with 500 µL 10% TCA followed by incubation on ice for 10 min to facilitate quantitative precipitation of the tRNA. After cooling, the reaction mixtures were transferred to glass microfiber filters and the tubes washed with 10% TCA to quantitate transfer. The filters were washed with additional cold 10% TCA followed by cold 95% ethanol. Filters were then transferred to scintillation vials, submerged in 5 mL of scintillation cocktail, and radioactivity measured by liquid scintillation counting. Assays involving transfer of the threonylcarbamoyl moiety activated by various nucleotides were performed as described above except that [^{14}C]-threonine (50 µM, 100,000 dpm/assay) was used as the radioactive label, unlabeled sodium bicarbonate (20 mM, pH 7.4) was added, and nucleotides were added to 3.0 mM. All of the assays were carried out in duplicate, and the data represent the results of at least three independent trials.

T. maritima t^6A assays with amino acids and nucleotides

Assays probing the transfer of *N*-carbamoyl amino acids (L-threonine, D,L-3-hydroxynorvaline, and serine), to tRNA via the *T. maritima* TCT complex were performed as described above for the *E. coli* TCT complex, except that assays were carried out at 60°C for 1 h and contained the *T. maritima* TsaC2 (4 µM) and the *T. maritima* TCT complex, either as a preisolated complex with a molar ratio of TsaBDE at 2:2:1 (2.0 µM) or the individual proteins at a concentration of 4.0 µM each. Assays involving transfer of the threonylcarbamoyl moiety activated by various nucleotides were performed as described above except that [^{14}C]-threonine (50 µM, 100,000 dpm/assay) was used as the radioactive label, unlabeled sodium bicarbonate (20 mM, pH 7.4) was added, and nucleotides were added to 3.0 mM. All of the assays were carried out in duplicate, and the data represent the results of at least three independent trials.

NMR analysis of amino acid binding to TsaC, TsaC2, and TsaD

For each STD-NMR experiment, a sample containing 20 µM protein (*E. coli* or *T. maritima* TsaC(C2) or TsaD) and 1 mM amino acid (L-threonine or D,L-3-hydroxynorvaline) was prepared in 500 µL 10 mM potassium phosphate pH 6.8, 100 mM NaCl, 99% D_2O. L-threonine ^{1}H assignments were obtained from the Biological Magnetic Resonance Bank (Ulrich et al. 2008); hydroxynorvaline assignments were made on the basis of chemical shift and observed signal splitting due to spin-spin coupling. The on-resonance irradiation of the protein during the 1D STD NMR experiment was performed at a chemical shift of −4.5 ppm where no amino acid resonances were present. Off-resonance irradiation was applied at 40 ppm. All spectra were obtained at 37°C with 1024 scans. The NMR data were processed and analyzed using Topspin 4.0.2 (Bruker).

SUPPLEMENTAL MATERIAL

Supplemental material is available for this article.

ACKNOWLEDGMENTS

This work was supported by National Institutes of Health grant R01 GM110588 to M.A.S., P.F.A., and D.I.-R., National Institutes of Health grant R01 GM70641 to V. de C.-L. and D.I.-R, and the California Metabolic Research Foundation to M.A.S.

Received April 3, 2020; accepted May 3, 2020.

REFERENCES

Boccaletto P, Machnicka MA, Purta E, Piatkowski P, Baginski B, Wirecki TK, de Crecy-Lagard V, Ross R, Limbach PA, Kotter A, et al. 2018. MODOMICS: a database of RNA modification pathways. 2017 update. *Nucleic Acids Res* **46:** D303–D307. doi:10.1093/nar/gkx1030

Bochner BR, Ames BN. 1982. Complete analysis of cellular nucleotides by two-dimensional thin layer chromatography. *J Biol Chem* **257:** 9759–9769.

Buckstein MH, He J, Rubin H. 2008. Characterization of nucleotide pools as a function of physiological state in *Escherichia coli*. *J Bacteriol* **190:** 718–726. doi:10.1128/JB.01020-07

Deutsch C, El Yacoubi B, de Crecy-Lagard V, Iwata-Reuyl D. 2012. Biosynthesis of threonylcarbamoyl adenosine (t^6A), a universal tRNA nucleoside. *J Biol Chem* **287:** 13666–13673. doi:10.1074/jbc.M112.344028

Lauhon CT. 2012. Mechanism of N6-threonylcarbamoyladenonsine (t^6A) biosynthesis: isolation and characterization of the intermediate threonylcarbamoyl-AMP. *Biochemistry* **51:** 8950–8963. doi:10.1021/bi301233d

Lin H, Miyauchi K, Harada T, Okita R, Takeshita E, Komaki H, Fujioka K, Yagasaki H, Goto YI, Yanaka K, et al. 2018. CO_2-sensitive tRNA modification associated with human mitochondrial disease. *Nat Commun* **9:** 1875. doi:10.1038/s41467-018-04250-4

Luthra A, Swinehart W, Bayooz S, Phan P, Stec B, Iwata-Reuyl D, Swairjo MA. 2018. Structure and mechanism of a bacterial t^6A biosynthesis system. *Nucleic Acids Res* **46:** 1395–1411. doi:10.1093/nar/gkx1300

Luthra A, Paranagama N, Swinehart W, Bayooz S, Phan P, Quach V, Schiffer JM, Stec B, Iwata-Reuyl D, Swairjo MA. 2019. Conformational communication mediates the reset step in t^6A biosynthesis. *Nucleic Acids Res* **47:** 6551–6567. doi:10.1093/nar/gkz439

Matuszewski M, Wojciechowski J, Miyauchi K, Gdaniec Z, Wolf WM, Suzuki T, Sochacka E. 2017. A hydantoin isoform of cyclic N^6-threonylcarbamoyladenosine (ct^6A) is present in tRNAs. *Nucleic Acids Res* **45:** 2137–2149. doi:10.1093/nar/gkw1189

Miyauchi K, Kimura S, Suzuki T. 2013. A cyclic form of N^6-threonylcarbamoyladenosine as a widely distributed tRNA hypermodification. *Nat Chem Biol* **9:** 105–111. doi:10.1038/nchembio.1137

Murphy FV, Ramakrishnan V, Malkiewicz A, Agris PF. 2004. The role of modifications in codon discrimination by $tRNA^{Lys}_{UUU}$. *Nat Struct Mol Biol* **11:** 1186–1191. doi:10.1038/nsmb861

Nagao A, Ohara M, Miyauchi K, Yokobori SI, Yamagishi A, Watanabe K, Suzuki T. 2017. Hydroxylation of a conserved tRNA modification establishes non-universal genetic code in echinoderm mitochondria. *Nat Struct Mol Biol* **24:** 778–782. doi:10.1038/nsmb.3449

O'Brien WE. 1976. A continuous spectrophotometric assay for argininosuccinate synthetase based on pyrophosphate formation. *Anal Biochem* **76:** 423–430. doi:10.1016/0003-2697(76)90337-7

Parthier C, Gorlich S, Jaenecke F, Breithaupt C, Brauer U, Fandrich U, Clausnitzer D, Wehmeier UF, Bottcher C, Scheel D, et al. 2012. The *O*-carbamoyltransferase TobZ catalyzes an ancient enzymatic reaction. *Angew Chem Int Ed Engl* **51:** 4046–4052. doi:10.1002/anie.201108896

Perrochia L, Crozat E, Hecker A, Zhang W, Bareille J, Collinet B, van Tilbeurgh H, Forterre P, Basta T. 2013. *In vitro* biosynthesis of a universal t^6A tRNA modification in Archaea and Eukarya. *Nucleic Acids Res* **41:** 1953–1964. doi:10.1093/nar/gks1287

Reddy DM, Crain PF, Edmonds CG, Gupta R, Hashizume T, Stetter KO, Widdel F, McCloskey JA. 1992. Structure determination of two new amino acid-containing derivatives of adenosine from tRNA of thermophilic bacteria and archaea. *Nucleic Acids Res* **20:** 5607–5615. doi:10.1093/nar/20.21.5607

Schweizer MP, McGrath K, Baczynskyj L. 1970. The isolation and characterization of N-[9-(β-D-ribofuranosyl)-purin-6-ylcarbamoyl]glycine from yeast transfer RNA. *Biochem Biophys Res Commun* **40:** 1046–1052. doi:10.1016/0006-291X(70)90899-5

Segel I. 1975. *Enzyme kinetics: behavior and analysis of rapid equilibrium and steady-state enzyme systems*. John Wiley & Sons, New York.

Stuart J, Gdaniec Z, Guenther R, Marszalek M, Sochacka E, Malkiewicz A, Agris P. 2000. Functional anticodon architecture of human $tRNA^{Lys3}$ includes disruption of intraloop hydrogen bonding by the naturally occurring amino acid modification, t^6A. *Biochemistry* **39:** 13396–13404. doi:10.1021/bi0013039

Thiaville PC, Iwata-Reuyl D, de Crecy-Lagard V. 2014. Diversity of the biosynthesis pathway for threonylcarbamoyladenosine (t^6A), a universal modification of tRNA. *RNA Biol* **11:** 1529–1539. doi:10.4161/15476286.2014.992277

Thiaville PC, El Yacoubi B, Kohrer C, Thiaville JJ, Deutsch C, Iwata-Reuyl D, Bacusmo JM, Armengaud J, Bessho Y, Wetzel C, et al. 2015. Essentiality of threonylcarbamoyladenosine (t^6A), a universal tRNA modification, in bacteria. *Mol Microbiol* **98:** 1199–1221. doi:10.1111/mmi.13209

Thiaville PC, Legendre R, Rojas-Benitez D, Baudin-Baillieu A, Hatin I, Chalancon G, Glavic A, Namy O, de Crecy-Lagard V. 2016. Global translational impacts of the loss of the tRNA modification t^6A in yeast. *Microb Cell* **3:** 29–45. doi:10.15698/mic2016.01.473

Ulrich EL, Akutsu H, Doreleijers JF, Harano Y, Ioannidis YE, Lin J, Livny M, Mading S, Maziuk D, Miller Z, et al. 2008. BioMagResBank. *Nucleic Acids Res* **36:** D402–D408. doi:10.1093/nar/gkm957

Yan Y, Zhang D, Zhou P, Li B, Huang SY. 2017. HDOCK: a web server for protein–protein and protein–DNA/RNA docking based on a hybrid strategy. *Nucleic Acids Res* **45:** W365–W373. doi:10.1093/nar/gkx407

Yu N, Jora M, Solivio B, Thakur P, Acevedo-Rocha CG, Randau L, de Crecy-Lagard V, Addepalli B, Limbach PA. 2019. tRNA modification profiles and codon-decoding strategies in *Methanocaldococcus jannaschii*. *J Bacteriol* **201:** e00690-18. doi:10.1128/JB.00690-18

Zhang W, Collinet B, Perrochia L, Durand D, van Tilbeurgh H. 2015. The ATP-mediated formation of the YgjD–YeaZ–YjeE complex is required for the biosynthesis of tRNA t^6A in *Escherichia coli*. *Nucleic Acids Res* **43:** 1804–1817. doi:10.1093/nar/gku1397